Fast neutron scattering on Gallium target at 14.8 MeV

R. Han[1,2,4], R. Wada[1], Z. Chen[1*], Y. Nie[3], X. Liu[1,4], S. Zhang[1,4], P. Ren[1,4],
B. Jia[1,4], G. Tian[1,4], F. Luo[1,4], W. Lin[1,4], J. Liu[1], F. Shi[1], M. Huang[1],
X. Ruan[3], J. Ren[3], Z. Zhou[3], H. Huang[3], J. Bao[3], K. Zhang[3], B. Hu[2]

[1]*Institute of Modern Physics, Chinese Academy of Sciences, Lanzhou, 730000, China*

[2]*School of Nuclear Science and Technology,*
Lanzhou University, Lanzhou 730000, China

[3]*China Institute of Atomic Energy, Beijing, 102413, China and*

[4]*University of Chinese Academy of Sciences, Beijing, 100049, China*

arXiv:1411.0403v1 [nucl-ex] 3 Nov 2014

Abstract

Benchmarking of evaluated nuclear data libraries was performed for $\sim$ 14.8 MeV neutrons on Gallium targets. The experiments were performed at China Institute of Atomic Energy(CIAE). Solid samples of natural Gallium (3.2 cm and 6.4 cm thick) were bombarded by $\sim$ 14.8 MeV neutrons and leakage neutron energy spectra were measured at 60° and 120°. The measured spectra are rather well reproduced by MCNP-4C simulations with the CENDL-3.1, ENDF/B-VII and JENDL-4.0 evaluated nuclear data libraries, except for the inelastic contributions around $E_n = 10 - 13$ MeV. All three libraries significantly underestimate the inelastic contributions. The inelastic contributions are further studied, using the Talys simulation code and the experimental spectra are reproduced reasonably well in the whole energy range by the Talys calculation, including the inelastic contributions.

Keywords: Neutron leakage spectra; Time-of-flight; Evaluated nuclear data; MCNP simulation; Talys code; Gallium

* zqchen@impcas.ac.cn

I. Introduction

The experimental studies of fast neutron scattering are important for design of nuclear reactors [1, 2]. They play a crucial role for verification of the evaluated nuclear data libraries, especially the elements that are of interest in accelerator driven systems, fission and fusion reactor technologies. Gallium (Ga) is one of such elements, which can be used as a cooling agent. Due to special physical properties of Ga, it is also used to make filling materials of some element samples, such as, Pu element within the device of reactors and nuclear weapons in a mixed form with Ga. Ga is a soft silvery metal and becomes liquid at slightly above the room temperature (29.78 °C). It is a moderate heat conductor similar to Lead and non-explosive unlike Sodium. Therefore it is a good candidate of a cooling agent for nuclear reactors. However, its available experimental data are limited and benchmarking of the evaluated nuclear data libraries is necessary. The benchmarking has been performed at CIAE since 2009 [3]. The validity of the benchmarking test system has been examined. Several targets have been studied, such as U [3], Be [4], water [5] and polyethylene [6].

In this article, we studied fast neutron scatterings on Ga samples. The leakage neutron energy spectra were measured by time of flight measurements and evaluated nuclear data libraries were benchmarked. The discrepancies between the experimental data and the simulations based on the evaluated nuclear libraries are further investigated. The article is organized as follows. In Sec.II, the experiment is briefly described. In Sec.III, the benchmarking of evaluated nuclear data libraries are presented. In Sec.IV, elastic and inelastic contributions are discussed. A summary is given in Sec.V.

II. Experiment

The experiment was performed at CIAE. Neutrons were produced by the $T(d,n)^4He$ reaction using the 300 keV D^+ beam accelerated by the Cockcroft-Walton accelerator. The average beam current was about 30 μA during the experiment. A silicon surface barrier detector positioned at 135° with respect to the D^+ beam was used to monitor the neutron yield by counting the associated ^4He particles. Another monitor, a BC501A scintillation detector, was placed at 7.98 m from the neutron source at approximately zero degree. The angles of the leakage neutrons are selected by changing the target position along the leakage

neutron direction, which results in change of the neutron emission angle from the Tritium target and the flight distance of the target sample to the detector. The energy distributions of the neutrons emitted from the $T(d,n)^4He$ source in different angles, 0°, 30°, 60° and 120° with respect to the D^+ beam direction, have been simulated using TARGET code [7]. The calculated results are shown in Fig. 1 with the experimentally observed distribution by the monitor scintillator near 0°. The energy distributions of the neutrons are around 14 MeV, slightly depending on different emission angles. The average neutron energy decreases slightly as the emission angle increases. The energy distribution measured by the monitor detector is well reproduced around the peak energy by the calculation at 0°, which is slightly affected by the accelerator pulse shapes. The pulse width of the D^+ beam during this experiment was kept $\sim$ 3 ns. In the experiment, the generated neutrons from two angles,

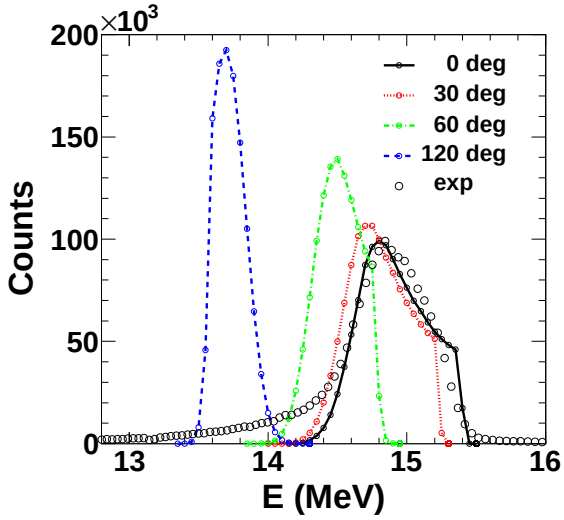

FIG. 1: Energy distributions of the neutrons emitted from the $T(d,n)^4He$ source in different angles (0°, 30°, 60° and 120°) with respect to the D^+ beam direction predicted by TARGET code. Open squares are the experimental distributions from the 0° monitor detector, which is normalized to the calculation at the peak value.

$-30°$ and 30° with respect to the D^+ beam direction were used, which gives the leakage neutron emission angle of 60° and 120°, respectively, and the same average incident neutron energy distribution peaked at around 14.8 MeV at both target positions. The beam was impinged on Ga samples. Natural Ga was used, which is composed of 60.11% ^{69}Ga and 39.89% ^{71}Ga. Two self-supported solid Ga samples were made as a cylindrical shape with ϕ13 cm × 3.2 cm and ϕ13 cm × 6.4 cm. (The samples were manufactured at a low temperature

room and stored in a refrigerator. During the experiment, room temperature was kept $\sim 20^{\circ}$ to keep them in solid.) Leakage neutron spectra from Gallium samples ware measured using a BC501A (ϕ5.08 cm $\times$ 2.54 cm) scintillation detector by a TOF technique with the flight path of 8.30 m and 8.67 m for 60° and 120°, respectively. A pre-collimator system, which is made of Iron, polyethylene and Lead, were orderly placed along the fight path between the sample and the detector. In front of the detector, another collimator was embedded inside the concrete wall of 2 m thick with a hole of $\sim$ 10 cm diameter , which was set to shield the neutron detector from background neutrons. Using such a heavy shielding and collimating system, high foreground/background ratio has been achieved. The light output function and the detection efficiency of the neutron detector were well calibrated at the 1-20 MeV at the Tandem Accelerator at CIAE [8]. For a given thresholds, the detection efficiency can be well determined with NEFF code [9]. Further details of the experimental setup and the data acquisition system can be found in Ref. [3] and [6].

III. Results

The neutron leakage time spectra measured in the experiment are shown by symbols in Fig. 2 (a) and (b). The measured data were normalized to the n-p scattering cross section on a polyethylene target in a separate run. Time calibration has been made, using the gamma peak which is eliminated in Fig. 2. The errors presented in the figure are from the statistical errors. As shown in the figure, the neutron leakage time spectra are quite similar with each other at both angles. Similar characteristic properties are also observed for those of the 3.2 cm thinner sample, and therefore their spectra are not shown. In the highest energy region, a shape peak is observed, which corresponds to the elastic scattering. The experimentally observed widths of the elastic peaks are dominated by the incident neutron energy distribution at the target which is shown in Fig.1. Inelastic contributions start right after the elastic peak. $(n, n'), (n, 2n), (n, np)$ and $(n, n\alpha)$ reaction channels are opened at the incident neutron energy of 14.8 MeV. These contributions are observed as a broad peak starting around 170 ns in the time spectra (below 13 MeV in energy).

To benchmark evaluated nuclear data libraries, the neutron leakage spectra are simulated by MCNP-4C [10] code using Gallium evaluated nuclear data from the CENDL3.1, ENDF/B-VII and JENDL4.0 libraries. In the MCNP simulations, the experimental parameters are

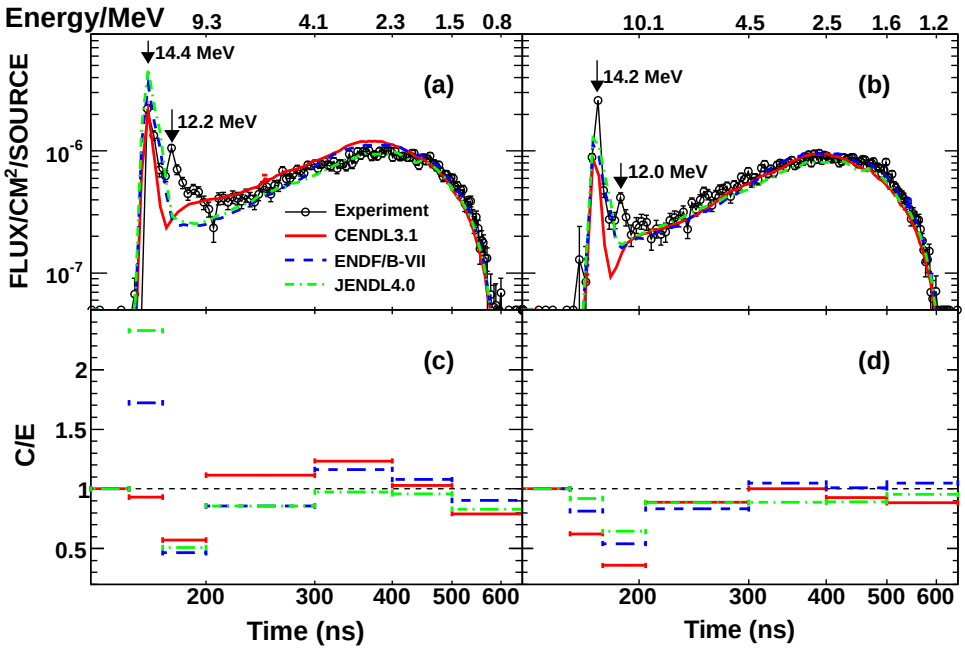

FIG. 2: Neutron leakage time spectra measured in the experiment and simulated by MCNP code at (a) 60° (b) 120° for 6.4-cm-thick gallium sample; Circles connected by line represent the experimental results, whereas different lines are those from the MCNP simulations using the evaluated databases of CENDL3.1 (solid), ENDF/B-VII (dashed) and JENDL4.0 (dot-dashed). The errors presented in the figure are from the statistical errors. (c) and (d) C/E ratios for CENDL3.1/experiment, ENDF/B-VII/experiment and JENDL4.0/experiment.

taken into account. These include the incident neutron energy distribution at the target, the target thickness, the neutron detection efficiency, the time response of the neutron detector and among others. The calculated results of the MCNP simulations are compared with those of the experiment in Fig. 2 (a) and (b). The general trends of the experimental neutron leakage spectra are well reproduced except for the inelastic peak around $E_n \sim 12$ MeV.

In order to make further detail comparisons, the ratios of calculated and experimental cross sections, C/E, are plotted in Fig. 2 (c) and (d) as a function of time for a certain time interval. From the above comparisons, we made the following observations:

1. At $t = 150 - 170$ ns ($E_n \sim 14$ MeV), a sharp elastic peak is observed. The simulated yield of the elastic scattering neutrons depends on the choice of the evaluated nuclear libraries. For 60°, the yield from the CENDL3.1 library agrees within 5% comparing

with that of the experiment, whereas those from the ENDF/B-VII and JENDL4.0 libraries are larger by a factor of ~ 1.8 and a factor of ~ 2.4, respectively. At 120°, the ratios are 0.6, 0.8, and 0.9 for the CEND3.1, ENDF/B-VII, and JENDL4.0, respectively.

2. At $t = 170 - 200$ ns ($E_n \sim 10 - 13$ MeV), a small, but clear peak is observed. The contribution originates from inelastic scatterings and all MCNP simulations using these three libraries do not show a peak as the experimental data do and significantly underestimate the cross section.

3. At $t > 200$ ns ($E_n < 10$ MeV), a broad peak is observed, which originates from the $(n, n'), (n, 2n), (n, np)$ and $(n, n\alpha)$ reaction channels. The experimental cross sections are well reproduced by the simulations from all three libraries within 20% at both angles.

IV. Discussions

In the following discussions, we first address the discrepancy of the elastic contribution for the different nuclear libraries. Then we address the problem of the inelastic contributions, using the Talys program.

A. Elastic contribution

The angular distributions of the elastic scattering for ^{69}Ga and ^{71}Ga, from the CENDL3.1, ENDF/B-VII and JENDL4.0 libraries, are shown in Fig. 3 (a) and (b), respectively. The available data of the three evaluated nuclear libraries at 14.75 MeV are used for the plots. As shown in Fig. 3 (a) and (b), the angular distributions show a strong forward peaking and an oscillation pattern appears at angles larger than 30°. The oscillation patterns of the evaluated elastic angular distributions of ^{69}Ga and ^{71}Ga from the CENDL3.1 and JENDL4.0 libraries are almost identical, whereas those from the ENDF/B-VII library show slightly different distributions between ^{69}Ga and ^{71}Ga. The elastic cross sections of ^{69}Ga and ^{71}Ga at 60° and 120°, are picked up from Fig. 3 (a) and (b), at angle positions indicated by arrows, and plotted in Fig. 3 (c) for 60° and (d) for 120° with the calculated values for the natural

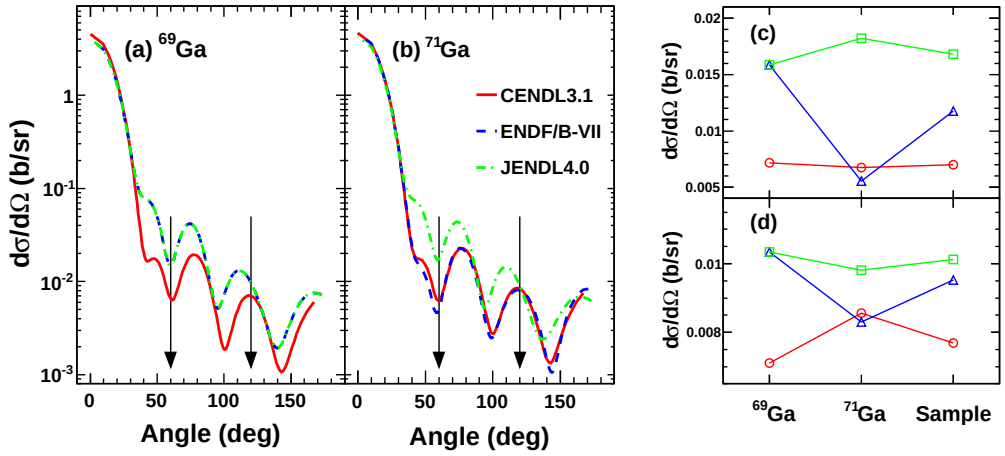

FIG. 3: Evaluated angular distributions of the elastic scattering channels for ^{69}Ga (a) and ^{71}Ga (b) given in the libraries of CENDL3.1, ENDF/B-VII and JENDL4.0. Different lines indicate different evaluated data from different libraries. Evaluated 60° (c) and 120° (d) elastic cross sections of ^{69}Ga, ^{71}Ga and natural sample from Fig. 3 (a) and (b) respectively.

Ga sample. One should note that 60° in the angular distribution locates near the valley of the distributions for all cases, and thus the effect of the ambiguity of the experimental angular determinations on the cross section becomes an order of less than 10%. 120°, on the other hand, locates near a peak for some cases. In this case the ambiguity from the angular determination becomes in the similar order, whereas for other cases, the angle locates on the shoulder of the distribution and thus the ambiguity becomes larger. The cross section of the natural target sample is calculated as $\sigma = 0.6011\sigma(^{69}Ga) + 0.3989\sigma(^{71}Ga)$. The ratios of the elastic cross sections of the target sample between these three libraries, are $\sigma_{CENDL3.1} : \sigma_{ENDF/B-VII} : \sigma_{JENDL4.0} \sim 1.0 : 1.7 : 2.4$ at 60° and $\sim 0.7 : 0.9 : 1.0$ at 120°. These ratios are quite consistent with those obtained in Fig. 2 (c) and (d), in which these ratios of 1.0 : 1.8 : 2.4 at 60° and 0.6 : 0.8 : 0.9 at 120° are obtained. These observations indicate that the discrepancies of the elastic scattering neutron yields in the MCNP simulations using the CENDL3.1, ENDF/B-VII and JENDL4.0 libraries in Fig. 2 (a) and (b) originate simply from the differences in the angular distribution of the elastic cross sections at 60° and 120° in these libraries. One should note that, as shown in Fig. 3 (a) and (b), the major contribution of the elastic scattering to the total reaction cross section is governed by the contribution at angles smaller than 30° and therefore the discrepancies

in the elastic peaks observed in this experiment is in a minor effect for the whole elastic contribution.

B. Inelastic contributions

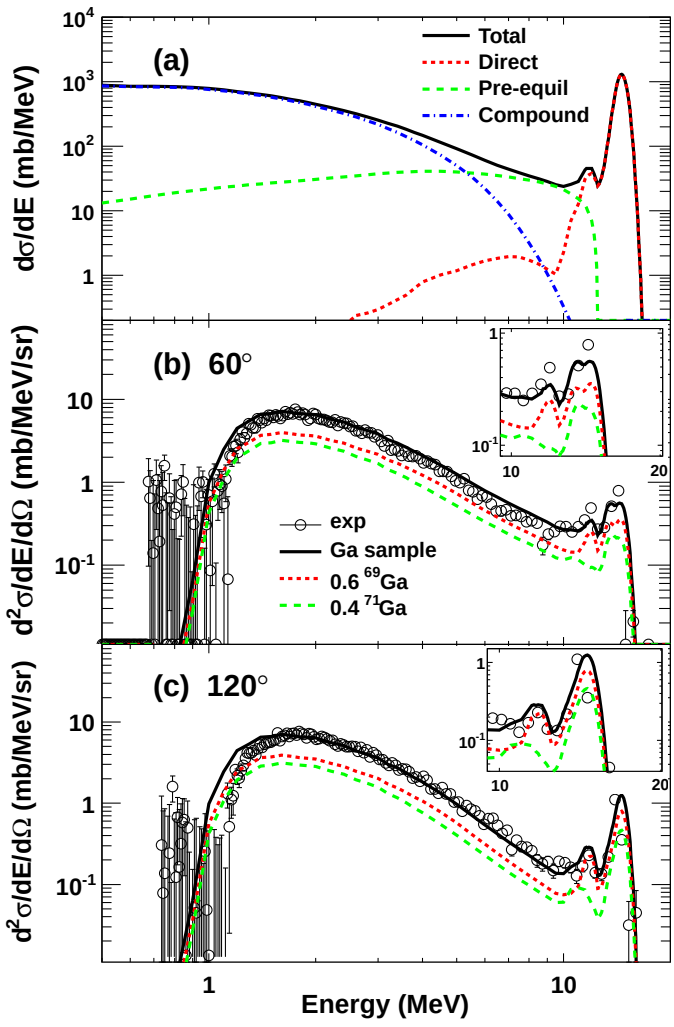

FIG. 4: (a) The total neutron leakage energy spectrum and the contributions from three processes (the direct, pre-equilibrium and compound processes) calculated by Talys code. The experimental spectra at 60° (b) and 120° (c) are compared with the Talys calculated for natural Ga, ^{69}Ga and ^{71}Ga, respectively. The detector efficiency has been considered in the Talys calculation. Insets show expanded energy spectra above 10 MeV.

To investigate the discrepancies in the neutron leakage energy spectra between the experiment and the MCNP simulations at $E_n \sim 10 - 13$ MeV, simulations by Talys-1.6 code [11]

are performed. In the Talys code, the neutron-induced reaction is divided in three physical processes, e.g., direct, pre-equilibrium and compound nucleus reactions. Calculated total neutron leakage energy spectrum and the contributions from three processes are shown in Fig. 4 (a). Natural Ga samples was used in the plots. The calculated total cross section show three characteristic features, an elastic peak, an inelastic peak and a broad bump in the low

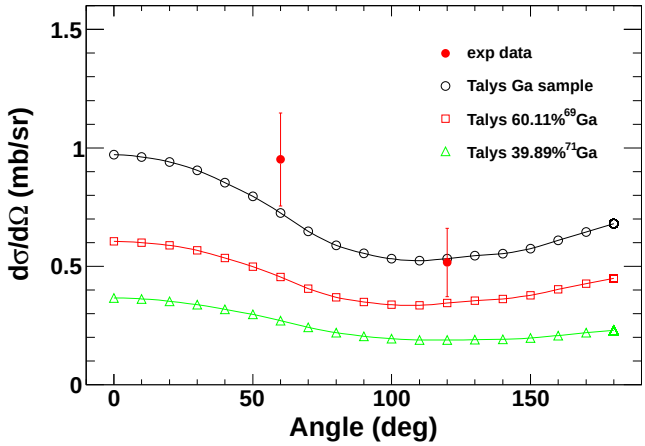

FIG. 5: Angular distribution the inelastic cross section integrated over $E_n = 10 - 12.5$ MeV from Talys simulations. The red dots are the experimental data for 60° and 120°.

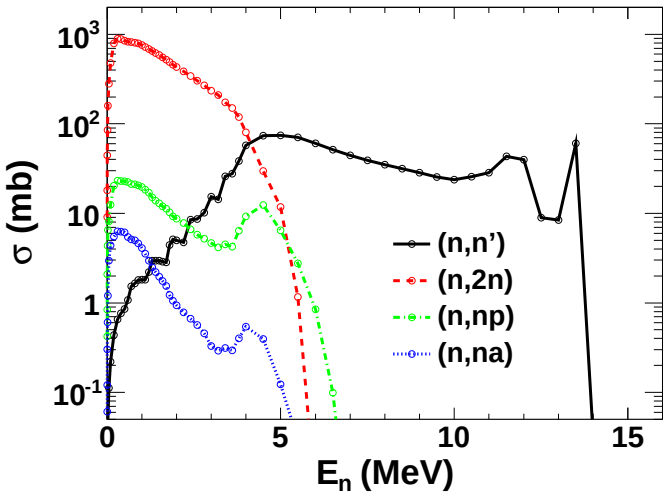

FIG. 6: The contributions of inelastic reaction from $(n, 2n), (n, np), (n, na)$ channels and a emission neutron in the continuum states $(0-12$ MeV) and discrete levels $(12-14$ MeV) from (n, n') channel in natural Ga sample. These results calculated by Talys code.

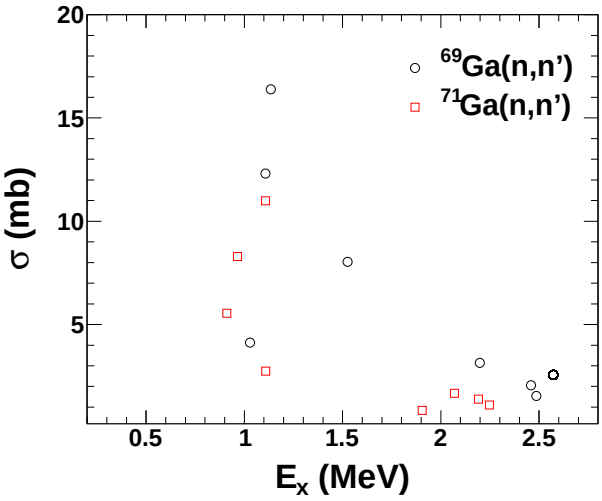

FIG. 7: Inelastic cross section of the leakage neutron from (n, n') channel in ^{69}Ga (circles) and ^{71}Ga (squares) as a function of E_x.

energy side. The elastic and inelastic peaks are generated by the direct process. The broad bump at the low energy is dominated by the compound nucleus process. The contribution from the pre-equilibrium process is dominated at the energy range of $E_n \sim 5 - 10$ MeV. In Fig. 4 (b) and (c), the experimental energy spectra at 60° and 120° are compared with the calculations, respectively. The experimental spectra are well reproduced by the calculated cross sections for the Ga sample, including the inelastic peaks at both angles. Individual contributions of ^{69}Ga and ^{71}Ga to those of the Ga sample are also shown by dotted and dashed lines. As shown clearly in the inserts, the inelastic peaks are mainly generated from the direct process of ^{69}Ga, but not of ^{71}Ga though a very small contribution from ^{71}Ga is observed at 120° at a slightly ($\sim$ 1 MeV) lower neutron energy. In Fig. 5 the calculated angular distribution of the inelastic cross section at $10.0 < E_n < 12.5$ MeV are plotted from the Talys simulation (open symbols) and compared with those of the experiment (filled circles). In contrast to the elastic channel, the calculated angular distribution is rather flat and the experimental data agree within the error bars at both angles. In this work, since we are focusing on the neutron emission channels, no neutron pick-up reaction channel is used in the direct reaction channel. In Fig. 6, the contributions of different reaction channels to the total reaction cross sections are plotted as a function of the leakage neutron energy for natural Ga sample. The (n, n') cross section is the sum of those from the discrete and continuum states calculations. The (n, n') channel dominates in the direct and pre-equilibrium contri-

bution at 5 MeV $\leq E_n \leq$ 12 MeV. At $E_n <$ 5 MeV, the compound nucleus contribution of the $(n, 2n)$ process is dominated and (n, np) and $(n, n\alpha)$ channels show minor contributions. In Fig. 7, the calculated cross section of the individual state below 2.6 MeV is plotted for ^{69}Ga(circles) and ^{71}Ga(squares). As one can see, the location of the excited levels are similar for the two isotopes, but the strengths are larger by about 50% for ^{69}Ga. For the natural Ga samples, the natural abundance of 40% is multiplied for ^{71}Ga and the relative yield to those of ^{69}Ga is further reduced. This causes a relatively small contribution from ^{71}Ga in the inelastic contribution at $E_n = 10 - 12$ MeV. This fact indicates that there is no essential difference between the reaction mechanisms of neutron scattering between ^{69}Ga and ^{71}Ga in the inelastic channels.

V. summary

The neutron leakage spectra from natural Ga samples at the incident energy of $\sim$ 14.8 MeV are compared with the MNCP simulations with the CENDL3.0, ENDF/B-VII and JENDL4.0 evaluated nuclear data libraries at 60° and 120°. The essential characteristic properties of the spectra are well reproduce by these simulations, except for the inelastic contributions at $E_n \sim$ 12 MeV. The results from all three libraries significantly underestimate the cross section in this energy range. The experimental spectra are further compared with those of the Talys simulations with the standard default parameters in addition to the parameters related to the experiments. The Talys simulations reproduce the experimental spectra very well, including the inelastic peak at $E_n \sim$ 12 MeV. It is found that the inelastic contributions originated mainly from the (n, n') channel of ^{69}Ga and minor contribution from those of ^{71}Ga. As far as concerning to the observed spectra for Ga samples in this experiment, the Talys code provides a slightly better nuclear data information, comparing to the CENDL3.0, ENDF/B-VII and JENDL4.0 evaluated nuclear data libraries.

Acknowledgments

The authors thank to the operational staff in the Cockcroft-Walton accelerator, China Institute of Atomic Energy, for their support during the experiment. The experiment is supported by the National Natural Science Foundation of China (Grants No. 11075189)

and ADS project 302 (Grants No. XDA03030200) of the Chinese Academy of Sciences.

[1] C. Steven and van der Marck, Nuclear Data Sheets. **113** (2012) 2935.

[2] Hiroyuki Hashikura *et al.*, Journal of Nuclear Science and Technology. **23**(6) (1986) 477.

[3] Y. Nie *et al.*, Annals of Nuclear Energy. **37** (2010) 1456.

[4] Y. Nie *et al.*, Annual Report of China Institute of Atomic Energy. (2013) 78.

[5] Zhang Kai *et al.*, Nuclear Techniques. **37**(8) (2014) 080501.

[6] Y. Nie *et al.*, Nuclear Physics Review. **29**(3) (2012) 310.

[7] D. Schlegel, TARGET User's Manual, laborbericht PTB-6.42-05-2. Braunschweig, Germany, 2005.

[8] H. X. Huang *et al.*, Chinese Physics C. **33**(8) (2009) 677.

[9] G. Dietze and H. Klein, NRESP4 and NEFF4 Monte Carlo Code for the Calculation of Neutron Response Functions and Detection Efficiencies for NE213 Scintillation Detectors. PTB-ND-22. Physikalisch-Technische Bundesanstalt, Braunschweig, Germany.

[10] J. Briesmeister, MCNPA General Monte Carlo N-particle Transport Code, Version 4C. Tech. Rep. LA 13709, M. Los Alamos National Laboratory, USA, 2000.

[11] A. Koning, S. Hilaire and S. Goriely, Nuclear Research and Consultancy Group, (2013), http://www.talys.eu/.